

1 **Mangrove sediment organic carbon storage and sources in relation to forest age**  
2 **and position along a deltaic salinity gradient**

3

4 Rey Harvey Suello<sup>1</sup>, Simon Lucas Hernandez <sup>1,5</sup>, Steven Bouillon<sup>2</sup>, Jean-Philippe Belliard<sup>1</sup>, Luis  
5 Dominguez-Granda<sup>3</sup>, Marijn Van de Broek<sup>4</sup>, Andrea Mishell Rosado Moncayo<sup>3</sup>, John Ramos Veliz<sup>3</sup>,  
6 Karem Pollette Ramirez<sup>3</sup>, Gerard Govers<sup>2</sup>, Stijn Temmerman<sup>1</sup>

7

8 <sup>1</sup> University of Antwerp, Ecosystem Management Research Group, <sup>2</sup> Katholieke Universiteit Leuven, Divi-  
9 sion of Soil and Water Management, <sup>3</sup> Escuela Superior Politecnica del Litoral, Department of Sustainable  
10 Water Management, <sup>4</sup> Swiss Federal Institute of Technology, Department of Environmental Systems Science,  
11 <sup>5</sup> Ghent University, Laboratory of Environmental Toxicology and Aquatic Ecology

12

13 Correspondence to: Rey Harvey Suello, Ecosystem Management Research Group (ECOBIE), University of  
14 Antwerp, Antwerp, Belgium (suello.reyharvey@uantwerpen.be)

15

16 **Abstract**

17

18 Mangroves are widely recognised as key ecosystems for climate change mitigation as they capture and  
19 store significant amounts of sediment organic carbon (SOC). Yet, there is incomplete knowledge on  
20 how sources of SOC and their differential preservation vary between mangrove sites in relation to envi-  
21 ronmental gradients. To address this, sediment depth profiles were sampled from mangrove sites ranging  
22 from river-dominated to marine-dominated sites and including old and young mangrove sites, in the  
23 Guayas delta (Ecuador). The stable carbon isotope ratios ( $\delta^{13}\text{C}$ ) and the elemental composition (OC%,  
24 C:N) of sediment profiles, local vegetation (i.e., autochthonous carbon) and externally-supplied sus-  
25 pended particulate matter (i.e., allochthonous carbon) were obtained to assess variations in the amount  
26 and sources of SOC at different locations throughout the delta. In general, across all sites, we found  
27 increasing SOC contents and stocks are associated with decreasing  $\delta^{13}\text{C}$  and increasing C/N ratios, indicating

28 that SOC stocks and sources are intrinsically related. The SOC stocks (down to 0.64 m [deep-depth](#) profiles)  
29 are significantly lower in young mangrove sites (46-55 Mg C ha<sup>-1</sup>) than in old sites (78 - 92 Mg C ha<sup>-1</sup>).  
30 The SOC in the young mangrove sites is mainly of allochthonous origin (estimated on average at 79%)  
31 whereas in the old sites there is a slight dominance of autochthonous OC (on average 59%). Moreover,  
32 from river- to marine-dominated sites, a pattern was found of increasing SOC stocks and increasing  
33 autochthonous SOC contribution. These observed differences along the two studied gradients are hy-  
34 pothesized to be mainly driven by (1) expected higher sedimentation rates in the river-dominated and  
35 lower-elevation younger sites, thereby ‘diluting’ the SOC content and decreasing the relative autoch-  
36 thonous contribution; and (2) potential differences in preservation of the different SOC sources. Our  
37 finding of high contributions of allochthonous SOC, especially in young mangroves, implies that this  
38 carbon is not originating from CO<sub>2</sub> sequestration by the mangrove ecosystem itself, but is externally  
39 supplied from other terrestrial, marine or estuarine ecosystems. We argue that accounting for lower SOC  
40 stocks and higher contribution of allochthonous SOC in young and river-dominated mangrove sites, as  
41 compared to old and marine-dominant sites, is particularly relevant for designing and valuing nature-  
42 based climate mitigation programs based on mangrove reforestation.

43

#### 44 KEYWORDS

45 blue carbon, sediment organic carbon, stable carbon isotope, autochthonous, allochthonous, climate change,  
46 Guayas delta

47

48

49

50

51

52

53

54

55

56 **1 | INTRODUCTION**

57

58 Situated at the interface between terrestrial and marine environments, mangrove forests are unique wetland  
59 ecosystems occupying (sub-)tropical intertidal zones (Burkett & Kusler, 2000; Duke et al., 2007; Polidoro et  
60 al., 2010; Tue et al., 2012). They provide a myriad of ecosystem services, such as their ability to contribute  
61 to global climate regulation by effectively sequestering carbon (Donato et al., 2011; Mcleod et al., 2011;  
62 Taillardat et al., 2018). Mangroves accumulate [organic](#) carbon at an estimated rate of 20-949 g C m<sup>-2</sup> yr<sup>-1</sup>,  
63 accounting for more than 10% of the carbon sequestration by the global ocean (Mcleod et al., 2011; Alongi,  
64 2014), while mangroves only cover ca. 2 % of the global ocean (Duarte et al., 2004). Compared to other  
65 ecosystem types, such as rain forests, peat swamps, salt marshes and seagrasses, mangroves store much  
66 higher carbon stocks which approximately range from 140 - 1023 Mg C ha<sup>-1</sup> (Donato et al., 2011; Alongi,  
67 2014; Schile et al., 2017). This demonstrates the importance of the carbon capture and storage capacity of  
68 mangrove ecosystems. Recent estimations by Atwood et al. (2017) equate to 2.6 billion Mg of C stored in  
69 mangrove sediments down to a 1 m depth worldwide.

70

71 This high capacity of mangroves to store carbon is to a large extent due to the accumulation of organic  
72 carbon into their sediments through a range of mechanisms. Generally, sediment organic carbon (SOC) orig-  
73 inates from autochthonous inputs (i.e. from local biomass production) and allochthonous inputs (i.e. from  
74 particulate sediment deposition during tidal inundation) that are well-preserved by the mostly anoxic sedi-  
75 ment conditions in mangroves (Kristensen [et al.](#), 2008). Above and belowground biomass accumulates in  
76 mangrove sediments through litterfall, vegetation die-off, root exudation, ~~and~~ root growth [and peat formation](#)  
77 ([Ezcurra et al., 2016](#)), and this constitutes the autochthonous SOC in mangrove sediments. On the other hand,  
78 during regular tidal flooding events mangroves trap allochthonous carbon from tidal waters containing fine  
79 sediment particles from marine, estuarine, and terrestrial origin (Alongi, 2014). These organic materials of  
80 both autochthonous and allochthonous origin are stored and buried in the mangrove sediments, through sed-  
81 imentation (during high tides and high-energy events like storm surges) and bioturbation (e.g. burrowing of  
82 crustaceans). The preservation of this buried SOC is dependent on, among other factors, organic matter sorp-  
83 tion to mineral substrates, microbial decomposition activity (Kristensen et al., 2008; Adame et al., 2015) and  
84 tide-driven groundwater fluxes (Maher et al., 2013).

85 Unveiling environmental gradients that affect variations in the amount of allochthonous and autochtho-  
86 nous SOC in mangroves is highly relevant, since the fate and long-term preservation of these two SOC  
87 sources may differ. Recent field studies in temperate-climate tidal marshes indicate that locally produced  
88 autochthonous SOC is abundantly present in the top 5-20 cm of sediment profiles, but is largely lost with  
89 increasing depth beneath the sediment surface, due to mineralization and leaching. In contrast, long-term  
90 preserved SOC is to a large extent of external allochthonous origin, suggesting this SOC source is more  
91 protected against mineralization (Van de Broek et al. 2018; Mueller et al. 2019). Furthermore, discriminating  
92 between autochthonous and allochthonous SOC sources is important, especially to properly assess the mag-  
93 nitude to which this ecosystem can help mitigate climate change. After all, it is only the autochthonous SOC  
94 that is assimilated from atmospheric CO<sub>2</sub> within the mangrove ecosystem itself, while the allochthonous SOC  
95 originates from externally supplied organic C from other upstream (terrestrial), downstream (marine) or es-  
96 tuarine ecosystems. In that respect, double accounting of allochthonous OC has to be avoided in carbon  
97 budgets (Van den Broek et al. 2018) as this SOC is originally sequestered in another environment. Yet the  
98 burial of allochthonous OC into mangrove SOC is relevant, as that OC may have contributed otherwise to  
99 greenhouse gas emissions from estuarine waters (Barr et al., 2010; Borges & Abril, 2011; Sturm et al., 2017;  
100 Jacotot et al. 2018). Thus, making a distinction between allochthonous and autochthonous SOC is crucial.  
101 However, there is limited knowledge on the relative contribution of the autochthonous and allochthonous  
102 inputs to SOC in mangroves and specifically how this contribution may vary spatially in relation to environ-  
103 mental gradients.

104  
105 The scarce number of studies on tidal marshes in temperate climate zones might provide hypotheses on  
106 which environmental gradients may be relevant for tropical mangroves. Here we focus on two gradients, for  
107 reasons argued below: (1) a deltaic or estuarine gradient from seaward sites (marine dominated) to landward  
108 sites (riverine dominated), and (2) young and old mangroves. Available studies from tidal marshes show a  
109 general pattern of decreasing SOC contents along estuarine salinity gradients from land to sea (Abril et al.,  
110 2002; Craft [et al.](#), 2007; Wieski et al., 2010; Hansen et al., 2017; Van de Broek et al., 2016), and this may  
111 be associated with shifts in the allochthonous versus autochthonous contributions to marsh SOC. For exam-  
112 ple, in studies of tidal marshes in the US (Craft [et al.](#), 2007) and in Belgium and the Netherlands (Van de

113 Broek et al., 2016), it was found that tidal marshes located more upstream along estuaries predominantly  
114 store SOC from allochthonous riverine inputs, due to higher contents of suspended particulate matter (SPM)  
115 and particulate organic carbon (POC), hence leading to higher rates of allochthonous SOC accumulation and  
116 higher SOC stocks in more upstream marsh sites. Further, young low-elevation marshes that established more  
117 recently on mudflats, are often characterized by higher rates of allochthonous sediment deposition, as com-  
118 pared to higher-elevation older marsh sites (Temmerman et al., 2004; Kirwan et al., 2016), and therefore it  
119 may be hypothesized that the SOC in young sites contains more allochthonous carbon as compared to old  
120 sites. However, it still remains to be investigated if such patterns on allochthonous versus autochthonous  
121 SOC sources and preservation, in relation to wetland age and position along an estuarine land-to-sea gradient,  
122 as found for temperate zone tidal marshes (Van de Broek et al., 2016; Van de Broek et al., 2018, Mueller et  
123 al., 2019), also occur in tropical mangroves, which obviously differ from marshes in many respects such as  
124 vegetation type, canopy density, and climate, among others.

125  
126 While it is widely accepted that mangroves act as major [carbon-C](#) sinks (Bouillon et al., 2008; Nelleman  
127 et al., 2009, Atwood et al., 2017; Marchand ~~et al.~~, 2017; Jennerjahn, 2020), at present, there are no studies  
128 that specifically investigated the stocks and sources of SOC in relation to the age and position of mangroves  
129 along the land-to-sea gradient within a delta or estuary. Therefore, this study aims at quantifying and identi-  
130 fying first-order controls of SOC stocks and sources (allochthonous versus autochthonous) along an estuarine  
131 land-to-sea gradient and between old and young mangrove forest sites, [for a specific case study](#) in the Guayas  
132 Delta, Ecuador.

133

## 134 **2 | MATERIALS AND METHODS**

135

### 136 **2.1 | Study site**

137

138 Field sampling was conducted in the Guayas Delta (Ecuador) which borders the Gulf of Guayaquil (Figure  
139 1), together forming the largest estuarine system along the Pacific coast of South America (Cucalon, 1989;  
140 Reynaud et al., 2018). Its geomorphology ~~consists of~~ [is characterized by](#) multiple branching river channels  
141 that intersect a large deltaic plain with approximately 4000 km<sup>2</sup> of mangroves (Reynaud et al., 2018). Tidal

142 gauge stations within the delta operated by Instituto Oceanográfico de la Armada del Ecuador (INOCAR,  
143 Oceanographic Institute of the Navy, Figure 1) recorded mean long-term (1984 -2016) tidal ranges of 2.12,  
144 2.85, and 3.42 m and sea level rise rates of 1.7, 4.9, and 4.0 mm/yr for stations Puerto Bolivar, Puná and Rio  
145 Guayas, respectively.

146

147 Two main estuarine sub-systems can be distinguished within the delta. To the east is the Guayas River  
148 estuary, which is a river-influenced estuary exhibiting a salinity gradient that ranges from 0-2 at the landward  
149 side of the tidal influence to 30 ppt at the delta mouth during the yearly dry season (June to November),  
150 dropping down at the latter location to 15-20 during the wet season (December to May) (Arreaga Vargas,  
151 2000). To the west is the Estero El Salado estuary, which is a former tributary of the Guayas River that is  
152 now disconnected from freshwater river discharge at its northern limit, making it a marine-dominated estua-  
153 rine system with salinity levels higher than in the Guayas River, ranging from 23.4 – 32.7 (Cifuentes et al.,  
154 1996; Twilley et al., 1998; Reynaud et al., 2018). Rainfall in the Guayas River catchment is seasonal, with  
155 95 % of precipitation occurring in the rainy season. As a result, the Guayas River has an average monthly  
156 discharge of 1400 m<sup>3</sup>/s, ranging from 200 m<sup>3</sup>/s in the dry season to 1600 m<sup>3</sup>/s in the rainy season, during a  
157 year of average precipitation (Cifuentes et al. 1996; Twilley et al., 2001).

158

159 Eight sampling locations (see Table S1 for coordinates) were identified in these two subsystems, consist-  
160 ing of four paired sets of young and old mangrove sites that are located nearby each other (Figure 1). These  
161 four pairs of young/old sites were situated in four sampling zones with different position in the delta. Three  
162 different sampling zones were selected along the Guayas River estuary. These three sampling zones are re-  
163 ferred to as the Upstream, Intermediate and Downstream zones (Figure 1). A fourth sampling zone was se-  
164 lected in the marine-dominated El Salado estuary, which is further referred to as the Marine zone. Based on  
165 an analysis of historical LANDSAT satellite images, we selected within each zone a young mangrove site  
166 (only emerging on satellite images at least after 1993 by mangrove establishment on initially bare mudflats)  
167 and an old mangrove site (visible as established mangroves on satellite images older than 1984). [Although](#)  
168 [the selected young sites can't be biologically categorized as young, for the purpose of this study, we will](#)  
169 [refer to these sites as 'young' as they are still significantly younger than their older counterparts.](#) There is a

170 strong dominance of *Rhizophora samoensis* in the old sites and *Avicennia germinans* in the young sites of  
171 the intermediate, downstream and marine zones, whereas the young and old sites of the upstream zone show  
172 high diversity of mangroves (*Rhizophora* and *Avicennia*) and an understory of freshwater plant species. Trees  
173 on the old sites have stem diameters mostly between 0.5 and 1 m, while on young sites this was mostly  
174 between 0.1 and 0.5 m, confirming we had selected contrasting old and young sites.

175

## 176 **2.2 | Sample collection**

177

178 Sediment cores were collected in September 2018 using cylindrical PVC tubes (0.10 m diameter), inserted  
179 manually down to a minimum depth of 0.64 m. At each site, 3 replicate sediment cores were sampled with  
180 an approximate maximum distance of 3 meters per coring location, resulting in a total of 24 sediment cores.  
181 Aboveground biomass samples (sun-shaded and sun-exposed green leaves, senescent leaves, leaf litter, live  
182 twigs and branches) were collected in the field on all sampling locations, as well as belowground biomass  
183 (light-colored roots) were manually sampled from the sediment cores in the lab, to represent autochthonous  
184 mangrove biomass. Surface water samples for determination of allochthonous suspended particulate organic  
185 carbon (POC) concentration were also collected from the river channels directly adjacent to each mangrove  
186 site with a 3 L Niskin bottle from just below the water surface and stored in 1 L opaque plastic bottles in a  
187 cool box filled with ice. Water samples were taken during a high water and low water campaign, both during  
188 the dry season (September 2018) and wet season (March 2019).

189

190 All samples (sediment and biomass) were transported and immediately frozen at the laboratory. The fro-  
191 zen sediment cores were mechanically sliced per centimeter, thawed and then oven-dried at 60°C for 48  
192 hours. Biomass samples were oven-dried using the same procedure. Total suspended matter (TSM) and POC  
193 content of the TSM were determined by filtering a known volume of water through pre-weighed and pre-  
194 combusted 47 mm and 25 mm Whatmann GF/F filters (nominal pore size 0.7 µm), respectively.

195

## 196 **2.3 | Sample analyses**

197

198 From each core, subsamples (i.e., slices of 0.01 m depth increments) were taken every 0.04 m. To obtain the  
199 sediment bulk density the samples were oven-dried at 60°C for 48 hours and were desiccated for 30-minutes  
200 to constant weight. Large pieces of living macroscopic vegetation residues (i.e., light colored roots) were  
201 then manually removed and kept as belowground biomass samples, while the remaining sediment samples  
202 were homogenized. All samples were treated with 10% HCl solution after weighing them into silver cups to  
203 remove carbonates, and were left overnight in an oven at 50°C. These were then analyzed for OC content,  
204 C:N ratios and  $\delta^{13}\text{C}$  using an Elemental Analyzer (Thermo EA 1110 coupled to a Thermo Delta V Advantage  
205 isotope ratio mass spectrometer). For the analysis of grain size distribution, subsamples were taken every  
206 0.08 m for each core and were analyzed using a LS I3 320 Laser Diffraction Particle Size Analyzer. The  
207 grain size was classified to fractions of clay ( $<2\mu\text{m}$ ), silt ( $<2-63\mu\text{m}$ ) and sand ( $>63\mu\text{m}$ ).

208  
209 Before analysis of the plant materials, the samples were pulverized using a mortar and pestle. The re-  
210 maining samples with harder composition were powdered using a mechanical ball mill or after treatment  
211 with liquid nitrogen. The ground samples were then weighed into tin cups. The filters used to collect POC in  
212 TSM samples, on the other hand were exposed to HCl fumes for 4 hours to remove inorganic carbon and  
213 dried at 50 °C overnight. Hereafter, filters were encapsulated in silver cups and stored in well plates. All plant  
214 materials and filters were analyzed for OC, C:N and  $\delta^{13}\text{C}$  using the same EA-IRMS setup as for the sediment  
215 core samples.

216

217

## 218 **2.4 | Data analysis**

### 219 **2.4.1 | OC Stocks Calculation**

220

221 For the analysis of depth profiles of OC%,  $\delta^{13}\text{C}$  and C:N ratios, all replicate cores were analyzed at 0.04 m  
222 depth intervals. As the replicate cores have varying sampling depths, depth profiles were analyzed up to a  
223 maximum common depth of 0.64 m for the three replicates per location. For the determination of OC stocks,  
224 continuous depth profiles of SOC content and bulk density were first obtained by linear interpolation. The  
225 OC density ( $\text{g cm}^{-3}$ ) was then obtained by multiplying the interpolated OC (%) and bulk density ( $\text{g cm}^{-3}$ )  
226 values. The total OC stocks ( $\text{Mg OC ha}^{-1}$ ) from each site were finally determined by summing up OC density

227 at all depth intervals and then multiplying the values by the depth interval (cm). Compaction during sample  
228 collection was taken into account in the calculation of OC stocks.

#### 229 **2.4.2 | Two End-Member Mixing Model**

230  
231 To identify the sources and examine the factors controlling the accumulation of [organic carbon](#)OC in man-  
232 grove sediments, two end-member mixing curves were made describing the relationship between OC% and  
233  $\delta^{13}\text{C}$  values, and between C/N and  $\delta^{13}\text{C}$  values. Organic carbon derived from local (autochthonous) and ex-  
234 ternal (allochthonous) inputs are expected to exhibit different  $\delta^{13}\text{C}$  values. With this, two end-members,  
235 namely the  $\delta^{13}\text{C}$  ratio of the POC of the estuarine waters (allochthonous component) and of the above and  
236 belowground vegetation biomass (autochthonous component), were considered. The input parameter values  
237 were calculated using averages of the POC and vegetation data. The definition of these components was  
238 necessary to calculate the expected  $\delta^{13}\text{C}$  values of sediments for a given C/N or OC%. The latter calculation  
239 was done using the equations derived by Bouillon *et al.*, (2003). First, the fraction of the bulk sediment which  
240 is from mangrove origin,  $X_{\text{mangrove}}$ , was calculated as:

$$241$$
$$242 \quad X_{\text{mangrove}} = \frac{C_{\text{sediment}} (\%) - C_{\text{allocht}} (\%)}{C_{\text{mangrove}} (\%) - C_{\text{allocht}} (\%)} \quad (1)$$

$$243 \quad 0 < X_{\text{mangrove}} < 1 \quad (1)$$

244  
245 Where  $C_{\text{sediment}}$ ,  $C_{\text{allocht}}$ , and  $C_{\text{mangrove}}$  corresponds to the OC content (%) of the sediment, of the alloch-  
246 thonous particulate organic carbon and of the autochthonous vegetation, respectively. The result obtained  
247 from the equation above was correspondingly used to calculate the fraction of OC in the sediment that is of  
248 autochthonous mangrove origin,  $X_{\text{mangroveC}}$  (%), as:

$$249$$
$$250 \quad X_{\text{mangroveC}} = \frac{X_{\text{mangrove}} - C_{\text{mangrove}} (\%)}{X_{\text{mangrove}} * C_{\text{mangrove}} (\%) + (1 - X_{\text{mangrove}}) * C_{\text{allocht}} (\%)} \quad (2)$$

$$0 < X_{mangroveC} < 1$$

Finally, the expected  $\delta^{13}\text{C}$  of the sediment organic matter,  $\delta^{13}\text{C}_{\text{sediment}} (\text{‰})$ , was calculated as:

$$\delta^{13}\text{C}_{\text{sediment}} (\text{‰}) = X_{mangroveC} * \delta^{13}\text{C}_{mangrove} (\text{‰}) + (1 - X_{mangroveC}) * \delta^{13}\text{C}_{allocht} (\text{‰}) \quad (3)$$

Where  $\delta^{13}\text{C}_{mangrove} (\text{‰})$  and  $\delta^{13}\text{C}_{allocht} (\text{‰})$  correspond to the stable carbon isotopic composition of the autochthonous mangrove vegetation and allochthonous estuarine POC, respectively. For the relationship between the sediment  $\delta^{13}\text{C}$  values and C:N ratios, similar equations were derived.

### 2.4.3 | Statistical Analyses

To test whether the OC%,  $\delta^{13}\text{C}$  and C:N significantly differed between the young and old sites, paired t-tests were performed. One-way Analysis of Variance (ANOVA) was used to test if the same parameters and the OC stocks were statistically significantly different between zones (upstream, intermediate, downstream, and marine). All data were checked for normality (Shapiro-Wilk) and homogeneity of variances (Levene's Test) with a level of significance of  $p < 0.05$ . Appropriate transformations (log & box cox) were performed for data that were not normally distributed and corresponding non-parametric tests (Mann-Whitney & Kruskal-Wallis) were employed for data that remained non normal after transformations. The data were analyzed using R programming (R Core Team, 2017).

## 3 | RESULTS

### 3.1 | Sediment organic carbon (SOC) depth profiles

The SOC contents of the sampled mangrove sediments varied considerably from 1.10 to 7.80% (Figure 2). The SOC contents of the old mangrove sites were significantly higher than for the young counterparts (Upstream: T-test,  $T(5)=4.76$ ;  $p < 0.005$ ; Intermediate: T-test,  $T(5)=11.68$ ;  $p < 0.05$ ; Downstream: T-test,  $T(5)=12.01$ ;  $p < 0.005$ ) (Fig. 2 and Table S2). On the other hand, the SOC contents of the young and old sites

278 in the Marine zone were not significantly different (T-test,  $T(5) = 2.59$ ;  $p > 0.05$ ). A general pattern of increas-  
279 ing SOC content was observed from Upstream to Downstream sites and the values were found to significantly  
280 differ between these sites (Kruskal-Wallis, Chi-Square=68.29;  $p < 0.001$ ) (Fig. 2 and Table S2). The SOC  
281 content for each site showed a relatively uniform distribution over depth (Figure 2), with some minor varia-  
282 tions with depth for certain sites (Intermediate Old, Downstream Old and Marine sites).

### 283 3.2 | Inventories of sediment organic carbon stocks

284 A direct comparison between sites was done after calculating the SOC stocks down to the maximum common  
285 depth of 0.64 m, showing SOC stocks varying between  $46.6 \pm 0.3$  and  $98.3 \pm 1.9$  Mg C ha<sup>-1</sup> (Figure 3 and  
286 Table S3 and Figure S1). First, the SOC stocks were significantly higher on old sites as compared to young  
287 sites (T-test,  $T(5) = 2.80$ ;  $p < 0.005$ ). Secondly, the SOC stocks were found to significantly increase (ANOVA,  
288  $F_{6,14} = 12.39$ ;  $P < 0.001$ ) from upstream to downstream, at least for the old sites (Figure 3 and Table S2). The  
289 young and old sites of the Marine zone had SOC stocks ( $97.74 \pm 1.52$  and  $92.7 \pm 0.93$  Mg C ha<sup>-1</sup>, respectively)  
290 that are comparable to the Intermediate and Downstream old mangrove sites.

291

### 292 3.4 | Stable carbon isotope ratios in sediments and potential sources

293 Figure 4A-D shows the  $\delta^{13}\text{C}$  values of SOC along the sediment depth profiles, together with the  $\delta^{13}\text{C}$  values  
294 of the above and belowground vegetation and POC of the adjacent water bodies. The sediment  $\delta^{13}\text{C}$  values  
295 of the sediment cores are 6-10‰ higher relative to the [average](#) vegetation of the sites (Table S2 [and](#) S4 [and](#)  
296 [S8](#)) and varied between -28.1 and -24.4‰. In contrast, the average  $\delta^{13}\text{C}$  values of the POC of the adjacent  
297 water bodies (circles) in the Upstream, Intermediate and Downstream sites were found to correspond closer  
298 to the sediment  $\delta^{13}\text{C}$  values, with the  $\delta^{13}\text{C}$  value of sedimentary OC being lower compared to values for  
299 riverine POC (Table S5). Furthermore,  $\delta^{13}\text{C}$  values of the older sites (at the Intermediate, Downstream and  
300 Marine sites) are more negative than the younger sites (Fig. 4; Table S2 and Figure S2). Comparison between  
301 the young and old sites revealed that these differences were statistically significant at the Upstream, Interme-  
302 diate and Downstream zones (T-test,  $T_5 = 2.78$ ,  $T_5 = 41.25$ , and  $T_5 = 89.48$ ;  $p < 0.005$ , respectively). A generally  
303 homogeneous pattern of  $\delta^{13}\text{C}$  values with depth was observed in all the sites, except the Upstream old site  
304 (Fig. 4A-D).

305

306

### 307 3.5 | Two end-member mixing model

308 The  $\delta^{13}\text{C}$  was plotted against the elemental ratios (C/N) and SOC content (%) of the sediments from all sites  
309 (Figures 5A and 5B). Figure 5A showed a negative correlation ( $r = -0.83$ ) between the  $\delta^{13}\text{C}$  values and the  
310 SOC content of the sediment samples. An inverse relationship ( $r = -0.78$ ) was also observed between C/N  
311 ratios and  $\delta^{13}\text{C}$  values (Figure 5B.). The SOC content and C/N of the POC from the suspended particulate  
312 matter of the adjacent estuarine waters were particularly low (1.45– 3.24% and 7.3 – 9.5, respectively) and  
313 corresponded to less negative  $\delta^{13}\text{C}$  values (-25.1 to -27.2‰). On the other hand, the SOC content and C/N of  
314 the vegetation samples were found to be higher (26.5 -47.6 % and 27.1 – 47.2, respectively) and were matched  
315 with lower  $\delta^{13}\text{C}$  values (-33.7 to -29.0‰).

316 Mixing model curves were calculated then from the data (Fig. 5). The average mixing curves (referred to  
317 as “mixing mid” in Fig. 5A and B) were obtained using the average observed POC and vegetation data as  
318 input values for the model parameters in equations 1-3. To account for the uncertainty of the parameter val-  
319 ues, they were also varied to obtain minimum and maximum mixing curves (“mixing min” and “mixing max”  
320 in Fig. 6A and B). After checking the degree of sensitivity of the resulting mixing curves to the variations in  
321 input values, a slight variation of values was applied ( $\delta^{13}\text{C}_{\text{allocht}}$  between -27.0 and -25.2‰,  $\delta^{13}\text{C}_{\text{mangrove}}$  be-  
322 tween -33.0 and -27‰,  $\text{OC}_{\text{sediment}}$  between 0.6 and 1.5%,  $\text{C:N}_{\text{mangrove}}$  between 42 and 60), resulting in the  
323 minimum and maximum mixing curves in Figures 5A and B.

324 [To account for the variability of the  \$\delta^{13}\text{C}\$  values of the different above- and belowground plant materials](#)  
325 [\(roots, leaves, branches, live, senescent, and surface litter, see supporting Table S8\) used as vegetation end-](#)  
326 [member, a one-factor-at-a-time \(OAT\) sensitivity analysis was performed and no significant changes in the](#)  
327 [mixing model results after linear regression was observed \(Figure S4, S5, S6 and S7\).](#) Overall the obtained  
328 mixing curves encompass the observed data reasonably well.

329

### 330 3.6 | Stable carbon isotope ratios in sediments and potential sources

331 Estimations on the relative contribution (%) of allochthonous and autochthonous origin to the SOC (Figure  
332 6, see Table S4 and S8 for specific values of all sites-) show that overall, the sampled mangrove sediments  
333 predominantly contain externally supplied allochthonous carbon (estimated at 65 %) rather than locally  
334 produced autochthonous carbon. Younger sites also have more allochthonous carbon ( $79 \pm 17$  %) whereas  
335 older sites have slightly more autochthonous carbon ( $59 \pm 8$  %) stored in the sediments. While the contribu-  
336 tion of allochthonous carbon was consistently higher for all sites, a general pattern of increasing contribu-  
337 tion of autochthonous carbon from the upstream to the downstream and marine zones was observed (Figure  
338 6).

339

## 340 **4 | DISCUSSION**

341

342 Despite widespread recognition of mangroves as key ecosystems for climate change mitigation through C  
343 capture and storage (Mcleod et al., 2011; Pendelton et al., 2012; Siikamäki et al., 2012; Murdiyarso *et al.*,  
344 2015), relatively limited knowledge is available on the variability in amounts and sources of sediment organic  
345 carbon in relation to environmental gradients within a system, such as mangrove age and position along an  
346 estuarine land-to-sea gradient. Our study on the Guayas delta (Ecuador) shows that SOC stocks and contents  
347 on old sites increase from river-dominated to marine-dominated sites and are generally lower in young sites  
348 as compared to old sites. Across all sites, increasing SOC contents are associated with decreasing  $\delta^{13}\text{C}$  and  
349 increasing C/N ratios. This suggests that the sources of SOC are predominantly of allochthonous origin for  
350 younger sites (on average 79%), while for older sites there is a slight dominance of autochthonous SOC origin  
351 (on average 59%). In the following section we explore potential mechanisms and hypotheses that may explain  
352 these observations, and we discuss implications for managing mangroves for carbon capture and storage.

353

### 354 **4.1 | SOC variability between young and old mangrove sites**

355

356 The majority of the old mangrove sites along the Guayas Delta had a significantly higher SOC stock and  
357 content than the young sites (Figure 2 and Figure 3). As a first potential explanation, we hypothesize this is

358 due to a SOC 'dilution effect' that is, as explained below, related to differences in suspended sediment ac-  
359 cretion rates between old and young mangrove sites. Several authors (Pethick, 1981; Allen, 1990; French,  
360 1993; Temmerman et. al., 2003; Kirwan et al. 2016) have shown that more recently formed (young) tidal  
361 marshes experience higher sediment accretion rates than their older counterparts. This is because new  
362 (young) marsh formation, through establishment of pioneer vegetation on initially unvegetated intertidal flats,  
363 starts at a lower elevation relative to mean sea level as compared to the higher elevation of established old  
364 marshes. Hence younger, lower-elevation marshes are subject to a higher tidal inundation frequency, depth  
365 and duration, and therefore higher rate of suspended sediment supply and deposition. Applying this analogy  
366 ~~in to~~ mangroves, it is therefore reasonable to assume that the sampled sediment profiles in our young man-  
367 grove sites (formed after 1984 by mangrove establishment on originally unvegetated intertidal flats) have  
368 accreted at higher rates than at the adjacent old mangrove sites (already established, based on analysis of  
369 remote sensing images, at least before 1984). We expect that the higher volume of tidally supplied sediment  
370 input in young sites largely consists of mineral suspended sediments that are relatively low in POC content  
371 (Duarte et al. 2004; Saintilan et al. 2013; Alongi, 2014). This is confirmed by our SPM samples, which  
372 showed a low POC content of 1.45 to 3.24 %. Higher suspended sediment accretion rates on young man-  
373 groves, would result then in a 'dilution effect' of the locally produced mangrove organic matter which typi-  
374 cally has higher OC content. In line with our findings, other studies have also suggested that the ~~organic~~  
375 ~~carbon~~OC stock in mangrove sediments increases linearly with the mangrove forest age as ~~biomass-derive-~~  
376 ~~autochthonous~~ C significantly increased in older compared to younger forests (Lovelock et al. 2010;  
377 Marchand 2017).

378  
379 Additionally, the higher frequency and duration of tidal inundation in the lower-elevated young mangrove  
380 sites is expected to promote more tidal currents that could cause export of POC from macroscopic origin  
381 (litter of leaves, twigs, ~~and~~ barks, ~~...~~) that could otherwise have been buried in the system. Furthermore, older  
382 mangrove sites generally have a denser tree canopy and root structure than young mangrove sites, which was  
383 shown by Alongi (2012) to hinder tidal export of litter from the forest sediment surface. It has also been  
384 proposed that the sediments of younger mangroves, with lower surface elevations and more frequent tidal  
385 inundations, are more often in less reducing conditions due to daily renewal of electron acceptors (e.g. man-  
386 ganese and iron) with tides and oxygen diffusion by the *Avicennia* root systems (Marchand et al. 2004, 2006).

387 These conditions may have also contributed to a faster rate of SOC decomposition in young sites as compared  
388 to more prevalent anoxic conditions in older mangrove stands, which may lead to a higher degree of SOC  
389 preservation and thus higher SOC stock in older mangrove sediments.

390

391 For all the young sites and Upstream old site, where SOC stocks are lower than the other old sites, the  
392 autochthonous contribution of local vegetation to the SOC was estimated to be very low (i.e.,  $20.7 \pm 13\%$  of  
393 the SOC). The allochthonous OC coming from the water column as suspended matter can be considered as  
394 the main source of OC found in sediments of these sites. This is supported by the less negative  $\delta^{13}\text{C}$  values  
395 of the SOC in these areas that ranged between  $-27.5$  and  $-24.4\text{‰}$  (Figure 4A-D) and lower C:N ratios of  $11.5$   
396 –  $14.9$  (Table S2) compared to the other older sites. Generally lower C:N ratios and higher freshwater input  
397 of organic matter could indicate faster decomposition, hence resulting in lower SOC contents and stocks  
398 (Leopold *et al.*, 2015). Therefore, our data suggest that the majority of the SOC in these sites is not produced  
399 from newly fixed  $\text{CO}_2$  by the local mangrove vegetation but rather from tidal deposition of material originat-  
400 ing from terrestrial, marine or estuarine reservoirs. [We observed comparable SOC stocks and contents at the](#)  
401 [young and old sites of the Upstream zone, as opposed to the lower SOC stocks in young sites compared to](#)  
402 [old sites of the Intermediate and Downstream zones. This may be to some extent attributed to differences in](#)  
403 [the successional stages of the vegetation in these different sites: in the intermediate and downstream zones](#)  
404 [\(with higher salinity\), the young sites are dominated by smaller trees of \*Avicennia germinans\* \(known as an](#)  
405 [earlier successional species\) and the old sites are grown by high stands of \*Rhizophora somoensis\* \(known as](#)  
406 [a later successional species\); while in the upstream zone \(with lower salinity\), the vegetation was similar on](#)  
407 [old and young sites, with mixtures of both \*Avicennia\* and \*Rhizophora\* and an understory of freshwater marsh](#)  
408 [species. Hence this may suggest that young and old sites in the upstream zone are in a similar vegetation](#)  
409 [successional stage, and therefore may have reached similar SOC stock levels; while in the intermediate and](#)  
410 [downstream zones, the young sites are in an earlier successional stage, where the SOC has reached yet lower](#)  
411 [levels as compared to the nearby old sites.](#)

412 Furthermore, the old mangrove sites of the Intermediate, Downstream and Marine sites have lower  $\delta^{13}\text{C}$   
413 values ( $-28.1$  to  $-26.5\text{‰}$ ) and higher C:N ratios ( $17.7$  –  $33.9$ ) compared to the young sites and the Upstream  
414 old site. In these sites, it is estimated that more than half ( $59 \pm 8\%$ ) of the SOC is of autochthonous origin  
415 indicating that a significant portion of locally produced organic matter is preserved in these areas. Other

416 mangrove forests wherein  $\delta^{13}\text{C}$  and C:N values of sediments closely match those of the mangrove roots and  
417 aboveground vegetation also reported a similar portion of mangrove-derived SOC of 58% (Kristensen *et al.*,  
418 2008). This relatively higher contribution of locally produced carbon to the mangrove SOC could explain  
419 why these sites have higher SOC contents and stocks than the young mangrove sites, as the OC content in  
420 organic material derived from mangrove vegetation is normally higher than that of the suspended sediments  
421 (Figure 5A).

422 Finally, it is important to note the comparable SOC stocks and contents of the young and old sites of the  
423 Marine zone. This is clearly due to the high SOC content in the upper 0.20 m of the younger sites which  
424 compensate for the lower SOC content deeper than 0.20 m, and which results in similar depth-averaged SOC  
425 content as in the older sites (Figure 2). Analyses of the cores showed that a high amount of macroscopic  
426 vegetation remains were found in the upper 0.20 m of the young Marine site cores.

427

#### 428 **4.2 | SOC variability along the estuarine land-to-sea gradient**

429 We observed SOC contents and stocks to generally increase from zones with low to high salinity (Figure 2  
430 and 3). Similar patterns were found in river-influenced estuarine mangrove forests in the Ganges-Brahmapu-  
431 tra Delta in the Indian Sundarbans (Donato *et al.*, 2011), the Pichavaram Mangrove in southeast India (Ranjan  
432 *et al.*, 2011) and the Mui Ca Mau National Park in the Mekong Delta, Vietnam (Tue *et al.*, 2014). A potential  
433 reason could be the higher input of riverine mineral-rich sediments in the more upstream locations of the  
434 delta, resulting in higher mineral sediment accretion rates in the lower salinity zones, and diluting the organic  
435 matter content in the mangrove sediments. In addition, we found a strong positive correlation (Pearson's  $r=$   
436 0.96) between the SOC content and C:N ratios (see Figure S3 and S4) of the mangrove sediments. This may  
437 suggest that the higher N contents in the more upstream and young sites may contribute to higher mineral-  
438 associated carbon and hence, lower SOC contents and stocks.

439

440 From Upstream to Downstream, the mangrove sediment  $\delta^{13}\text{C}$  values closely match those of the POC  
441 from the estuarine waters, while  $\delta^{13}\text{C}$  values of the local vegetation biomass differ significantly from the  
442 sediment  $\delta^{13}\text{C}$  values (Figure 4A-D; Figure 5A and B). This suggests that the SOC in the studied mangroves  
443 along the land-to-sea gradient mainly consists of allochthonous sources (estimated at  $65 \pm 22\%$ ), while

Formatted: Font: Not Italic

444 preservation of locally produced autochthonous OC into SOC is limited. Fairly similar ranges of  $\delta^{13}\text{C}$  (-29.5  
445 to -23.9 ‰) and C:N (9 – 26.6) were obtained in the estuarine mangrove of Segara Anakan Lagoon in south-  
446 ern Java, Indonesia (Kusumaningtyas *et al.*, 2019; Jennerjahn 2021), where the majority of the organic matter  
447 in the mangrove sediment was also concluded to be externally derived. Additionally, a study of Weiss *et al.*  
448 (2016) in the Berau estuary in eastern Kalimantan, Indonesia, also found silt loam sediments (similar to the  
449 sediment texture found in the Guayas mangroves, Table S6) mainly composed of externally-derived OC  
450 which had a bulk density (0.4- 0.7 g cm<sup>-3</sup>) and  $\delta^{13}\text{C}$  values (-29.5 to -25.6‰) close to those found in our study  
451 (see Table S2).

452 A potential explanation to this observed predominance of externally derived SOC is the tidal range and  
453 the quality of the allochthonous and autochthonous organic matter that comes in the Guayas mangrove eco-  
454 systems. A study of the contribution of both internal and external inputs of OC in marsh sediments in the  
455 Scheldt Estuary, in the Netherlands and Belgium (Van de Broek *et al.*, 2016; Van de Broek *et al.*, 2018),  
456 proposed that the burial efficiencies of the different sources of POC are related to their decomposability. For  
457 this study area, they suggest that allochthonous POC is composed largely of terrestrial, recalcitrant POC.  
458 Consequently, allochthonous POC is expected to decompose relatively slower after burial and remain in  
459 sediments for a longer time. In contrast, they argue that the autochthonous POC, derived from local vegeta-  
460 tion, is fresh and labile, thus expected to decompose more rapidly than allochthonous recalcitrant POC. Such  
461 a difference in the quality of OC sources may potentially explain why there is a lower contribution of autoch-  
462 thonous OC in mangrove sediments of our study sites. As the Guayas system has a high tidal range of 3-5 m,  
463 this specific environmental condition may allow better drainage of the mangrove sediments during low tides,  
464 enabling deeper aeration of sediment profiles, and hence resulting in higher decomposition rates and less  
465 preservation of more labile OC from the local vegetation. In addition, we could visually observe that our  
466 study site is heavily bioturbated by red crabs (*Ucides occidentalis*) which may aerate the soil and could  
467 potentially lead to less preservation of autochthonous organic matter.

### 469 4.3 | Downcore variations of organic matter composition

470 In general, the individual SOC content,  $\delta^{13}\text{C}$  and C:N depth profiles (Figures 2 and 4 and Figure S2 and S3)  
471 of each site are relatively uniform. This can be potentially explained by the bioturbation effect of red crabs

472 that were abundantly present in the mangrove sampling areas (visible as burrowing holes and small mounds  
473 of burrowed material on top of the sediment surface). The active digging and maintenance of burrows by  
474 crabs, to escape from predation and from extreme environmental settings (Kristensen, 2007), may be ex-  
475 pected to mix the upper column of the mangrove sediments, making the profile almost vertically homoge-  
476 nous.

477 The old mangrove sites in the Intermediate, Downstream and Marine zones showed a limited but gradual  
478 increase in SOC content (Figure 2B-D) from the top layer down to 60 cm, which is accompanied by downcore  
479 increases in OC density (Figure S2). According to Kusumaningtyas *et al.* (2019), such pattern may be an  
480 indication of predominance of autochthonous mangrove organic matter in sediments originating from below-  
481 ground OC input (i.e. root material). The fact that we find such pattern in old sites, and not in young ones,  
482 could further support the finding of higher contribution of autochthonous sources to SOC in our old mangrove  
483 sites.

484

#### 485 **4.4 | Implications for management of mangrove forests as carbon sinks**

486 This study estimates that large fractions of the mangrove SOC come from allochthonous sources, which are  
487 originating from CO<sub>2</sub> that has been sequestered in other ecosystems (terrestrial, estuarine and/or marine) and  
488 transported and deposited in the mangroves. Additionally, these could also be old-aged carbon, already se-  
489 questered for a significant amount of time (Van de Broek *et al.*, 2018). This would imply that contemporary  
490 carbon capture by the mangrove ecosystem itself, contributes only partly and relatively little to long-term  
491 SOC storage. This finding is particularly relevant for budgeting the potential of mangrove ecosystems to  
492 mitigate climate change under nature-based mitigation programs such as PES and REDD+ (Yee, 2010; Loca-  
493 telli *et al.*, 2014; Nam *et al.*, 2015). As a consequence, relying on estimates of total SOC stocks in mangroves,  
494 may seriously overestimate the contribution of mangroves to contemporary CO<sub>2</sub> sequestration by the man-  
495 grove ecosystem itself.

496 We found that older mangroves store larger amounts of SOC than younger mangroves. This may suggest  
497 the importance of conservation of especially old-grown mangroves and, while measures to promote the for-  
498 mation of new young mangroves are still useful, it may provide less carbon storage on short-term as compared  
499 to old mangroves. How long it takes before young mangroves reach SOC contents and stocks similar to old

Formatted: Font: Not Italic

500 mangroves remains unknown. However, it is important to mention that sediment accretion rates may be  
501 higher on young than old mangroves, for reasons discussed above (see 4.1), which could partly compensate  
502 for the lower SOC contents of young mangroves, and therefore SOC accumulation rates may be more similar  
503 between young and old mangroves.

504 Our results also show that SOC contents and stocks in old mangroves increase from river- to marine-  
505 dominated sites. This suggests that conservation and expansion of mangroves in the marine-dominated part  
506 of estuaries may be most effective for carbon storage policies. However, sediment accretion rates may be  
507 higher in river-dominated sites which could lead to similar SOC accumulation rates with marine-dominated  
508 sites. Hence further research on linking sediment accretion and SOC accumulation rates, [which were not](#)  
509 [measured in this study](#), are imperative to shed light to these uncertainties.

510

## 511 **5 | CONCLUSIONS**

512 Our findings show strong indications that the age of the mangrove stand as well as its position along the land-  
513 to-sea gradient play a vital role in the amount and sources of carbon stored in the mangrove sediments in the  
514 Guayas delta (Ecuador). Young mangroves are found to have lower SOC contents and stocks than old man-  
515 groves. This may be potentially due to higher mineral-rich sediment inputs on initially lower elevated,  
516 younger mangroves, which dilutes the SOC content in the mangrove sediments. A pattern of increasing SOC  
517 stocks (and corresponding SOC content) from river- to marine-dominated sites was also found, which may  
518 be attributed to a similar dilution effect, where higher riverine mineral-rich sediment inputs lead to lower  
519 SOC contents on more river-dominated, lower salinity sites. Based on  $\delta^{13}\text{C}$  values and elemental C:N ratios,  
520 we identified that the SOC of the young mangrove sites is predominantly of allochthonous composition ( $79$   
521  $\pm 13\%$ ) whereas the old sites had only a slight dominance of autochthonous SOC ( $59 \pm 8\%$ ). Finally, our  
522 study highlights that only a portion of the SOC stored in mangrove ecosystems is originating from con-  
523 temporary  $\text{CO}_2$  sequestration by the ecosystem itself, which is particularly relevant to consider when  
524 designing and valuing nature-based climate mitigation programs based on mangrove reforestation.

525

## 526 **Funding Information**

527 Fonds Wetenschappelijk Onderzoek – Vlaanderen (FWO, Research Foundation Flanders, PhD grant no.  
528 FWO R.H.S., 1168520N and FWO project grant no. G060018N), Vlaamse Interuniversitaire Raad -  
529 Universitaire Ontwikkelingssamenwerking (VLIR-UOS), ActUA Prijs – University of Antwerp

530

## 531 REFERENCES

532 Abril, G., Nogueira, M., Etcheber, H., Cabeçadas, G., Lemaire, E., & Brogueira, M. J. (2002). Behaviour of  
533 organic carbon in nine contrasting European estuaries. *Estuarine, coastal and shelf science*, 54(2), 241-262.

534 Adame, M. F., Santini, N. S., Tovilla, C., Vázquez-Lule, A., Castro, L., & Guevara, M. (2015). Carbon stocks  
535 and soil sequestration rates of tropical riverine wetlands. *Biogeosciences*, 12(12), 3805-3818.

536 Allen, J. R. L. (1990). Salt-marsh growth and stratification: a numerical model with special reference to the  
537 Severn Estuary, southwest Britain. *Marine Geology*, 95(2), 77-96.

538 Alongi, D. M. (2012). Carbon sequestration in mangrove forests. *Carbon management*, 3(3), 313-322.

539 Alongi, D. M. (2014). Carbon cycling and storage in mangrove forests. *Annual review of marine science*, 6,  
540 195-219.

541 Arreaga Vargas, P. (2000). Análisis del comportamiento de la salinidad (intrusión salina) en el sistema Río  
542 Guayas Canal de Jambelí como parte del cambio climático.

543 Atwood, T. B., Connolly, R. M., Almahsheer, H., Carnell, P. E., Duarte, C. M., Lewis, C. J. E., ... & Serrano,  
544 O. (2017). Global patterns in mangrove soil carbon stocks and losses. *Nature Climate Change*, 7(7), 523.

545 Barr, J. G., Engel, V., Fuentes, J. D., Zieman, J. C., O'Halloran, T. L., Smith, T. J., & Anderson, G. H. (2010).  
546 Controls on mangrove forest-atmosphere carbon dioxide exchanges in western Everglades National Park.  
547 *Journal of Geophysical Research: Biogeosciences*, 115(G2).

548 Borges, A.V. & Abril, G. (2011) Carbon Dioxide and Methane Dynamics in Estuaries. In: Wolanski E,  
549 McLusky DS (eds) *Treatise on Estuarine and Coastal Science*, vol 5. Academic Press, Waltham, 119–161.

550 Bouillon, S., Dahdouh-Guebas, F., Rao, A. V. V. S., Koedam, N., & Dehairs, F. (2003). Sources of organic  
551 carbon in mangrove sediments: variability and possible ecological implications. *Hydrobiologia*, 495(1-3),  
552 33-39.

553 Bouillon, S., Borges, A. V., Castañeda-Moya, E., Diele, K., Dittmar, T., Duke, N. C., ... & Rivera-Monroy,  
554 V. H. (2008). Mangrove production and carbon sinks: a revision of global budget estimates. *Global Biogeo-*  
555 *chemical Cycles*, 22(2).

556 Burkett, V., & Kusler, J. (2000). Climate change: potential impacts and interactions in wetlands of the united  
557 states I. *JAWRA Journal of the American Water Resources Association*, 36(2), 313-320.

558 Cifuentes, L. A., Coffin, R. B., Solorzano, L., Cardenas, W., Espinoza, J., & Twilley, R. R. (1996). Isotopic  
559 and elemental variations of carbon and nitrogen in a mangrove estuary. *Estuarine, Coastal and Shelf Science*,  
560 43(6), 781-800.

561 Craft, C. (2007). Freshwater input structures soil properties, vertical accretion, and nutrient accumulation of  
562 Georgia and US tidal marshes. *Limnology and oceanography*, 52(3), 1220-1230.

563 [Cruz-Orozeo, R. \(1974\). Morphodynamics and sedimentation of the Rio Guayas delta, Ecuador.](#)

564 Cucalón, E. (1989). Oceanographic characteristics off the coast of Ecuador. A sustainable shrimp mariculture  
565 industry for Ecuador, pp. University of Rhode Island, Narragansett, RI: Coastal Resources Center.

566 Donato, D. C., Kauffman, J. B., Murdiyarto, D., Kurnianto, S., Stidham, M., & Kanninen, M. (2011). Man-  
567 groves among the most carbon-rich forests in the tropics. *Nature geoscience*, 4(5), 293.

568 Duarte, C. M., Middelburg, J. J., & Caraco, N. (2004). Major role of marine vegetation on the oceanic carbon  
569 cycle. *Biogeosciences discussions*, 1(1), 659-679.

570 Duke, N.C., Meynecke, J.O., Dittmann, S., Ellison, A.M., Anger, K. et al. (2007). A world without man-  
571 groves. *Science* 317: 41.

572 [Ezcurra, P., Ezcurra, E., Garcillán, P. P., Costa, M. T., & Aburto-Oropeza, O. \(2016\). Coastal landforms and](#)  
573 [accumulation of mangrove peat increase carbon sequestration and storage. \*Proceedings of the National Acad-\*](#)  
574 [\*emy of Sciences\*, 113\(16\), 4404-4409.](#)

575 French, J. R. (1993). Numerical simulation of vertical marsh growth and adjustment to accelerated sea-level  
576 rise, north Norfolk, UK. *Earth Surface Processes and Landforms*, 18(1), 63-81.

Formatted: French (Belgium)

577 Hansen, K., Butzeck, C., Eschenbach, A., Gröngröft, A., Jensen, K., & Pfeiffer, E. M. (2017). Factors influ-  
578 encing the organic carbon pools in tidal marsh soils of the Elbe estuary (Germany). *Journal of soils and*  
579 *sediments*, 17(1), 47-60.

580 Jacotot, A., Marchand, C., & Allenbach, M. (2018). Tidal variability of CO<sub>2</sub> and CH<sub>4</sub> emissions from the  
581 water column within a *Rhizophora* mangrove forest (New Caledonia). *Science of the Total Environment*,  
582 631, 334-340.

583 Jennerjahn, T. C. (2020). Relevance and magnitude of 'Blue Carbon' storage in mangrove sediments: Carbon  
584 accumulation rates vs. stocks, sources vs. sinks. *Estuarine, Coastal and Shelf Science*, 247, 107027.

585 Jennerjahn, T. C. (2021). Relevance of allochthonous input from an agriculture-dominated hinterland for  
586 "Blue Carbon" storage in mangrove sediments in Java, Indonesia. In *Dynamic Sedimentary Environments*  
587 *of Mangrove Coasts* (pp. 393-414). Elsevier.

588 Kirwan, M. L., Temmerman, S., Skeeahan, E. E., Guntenspergen, G. R., and Fagherazzi, S. (2016). Overesti-  
589 mation of marsh vulnerability to sea level rise: *Nature Climate Change*, v. 6, p. 253-260.

590 Kristensen, E. (2007). Mangrove crabs as ecosystem engineers; with emphasis on sediment processes. *Jour-*  
591 *nal of sea Research*, 59(1-2), 30-43.

592 Kristensen, E., Bouillon, S., Dittmar, T., & Marchand, C. (2008). Organic carbon dynamics in mangrove  
593 ecosystems: a review. *Aquatic botany*, 89(2), 201-219.

594 Kusumaningtyas, M. A., Hutahaean, A. A., Fischer, H. W., Pérez-Mayo, M., Ransby, D., & Jennerjahn, T.  
595 C. (2019). Variability in the organic carbon stocks, sources, and accumulation rates of Indonesian mangrove  
596 ecosystems. *Estuarine, Coastal and Shelf Science*, 218, 310-323.

597 Leopold, A., Marchand, C., Deborde, J., & Allenbach, M. (2015). Temporal variability of CO<sub>2</sub> fluxes at the  
598 sediment-air interface in mangroves (New Caledonia). *Science of the Total Environment*, 502, 617-626.

599 Locatelli, T., Binet, T., Kairo, J. G., King, L., Madden, S., Patenaude, G., ... & Huxham, M. (2014). Turning  
600 the tide: how blue carbon and payments for ecosystem services (PES) might help save mangrove forests.  
601 *Ambio*, 43(8), 981-995.

602 Lovelock, C. E., Sorrell, B. K., Hancock, N., Hua, Q., & Swales, A. (2010). Mangrove forest and soil devel-  
603 opment on a rapidly accreting shore in New Zealand. *Ecosystems*, 13(3), 437-451.

604 Maher, D. T., Santos, I. R., Golsby-Smith, L., Gleeson, J., & Eyre, B. D. (2013). Groundwater-derived dis-  
605 solved inorganic and organic carbon exports from a mangrove tidal creek: The missing mangrove carbon  
606 sink?. *Limnology and Oceanography*, 58(2), 475-488.

607 Marchand, C., Baltzer, F., Lallier-Vergès, E., & Albéric, P. (2004). Pore-water chemistry in mangrove sedi-  
608 ments: relationship with species composition and developmental stages (French Guiana). *Marine Geology*,  
609 208(2-4), 361-381.

610 Marchand, C., Lallier-Vergès, E., Baltzer, F., Albéric, P., Cossa, D., & Baillif, P. (2006). Heavy metals dis-  
611 tribution in mangrove sediments along the mobile coastline of French Guiana. *Marine chemistry*, 98(1), 1-  
612 17.

613 Marchand, C. (2017). Soil carbon stocks and burial rates along a mangrove forest chronosequence (French  
614 Guiana). *Forest ecology and management*, 384, 92-99.

615 Mcleod, E., Chmura, G. L., Bouillon, S., Salm, R., Björk, M., Duarte, C. M., ... & Silliman, B. R. (2011). A  
616 blueprint for blue carbon: toward an improved understanding of the role of vegetated coastal habitats in  
617 sequestering CO<sub>2</sub>. *Frontiers in Ecology and the Environment*, 9(10), 552-560.

618 Mueller, P., Ladiges, N., Jack, A., Schmiedl, G., Kutzbach, L., Jensen, K., ~~and~~ & Nolte, S. (2019). Assessing  
619 the long-term carbon-sequestration potential of the semi-natural salt marshes in the European Wadden Sea:  
620 *Eco-sphere*, v. 10, no. 1.

621 Murdiyarso, D., Purbopuspito, J., Kauffman, J. B., Warren, M. W., Sasmito, S. D., Donato, D. C., ... &  
622 Kurnianto, S. (2015). The potential of Indonesian mangrove forests for global climate change mitigation.  
623 *Nature Climate Change*, 5(12), 1089.

624 Nam, M. V. (2015). *Mangroves for the Future Phase III–National Strategic Action Plan (2015–2018)*.

625 [Nellemann, C., Corcoran, E., Duarte, C. M., Valdés, L., De Young, C., Fonseca, L., & Grimsditch, G. \(2009\).](#)  
626 [Blue carbon. A Rapid Response Assessment. United Nations Environment Programme, GRID-Arendal, 78.](#)

627 Pendleton, L., Donato, D. C., Murray, B. C., Crooks, S., Jenkins, W. A., Sifleet, S., ... & Megonigal, P.  
628 (2012). Estimating global “blue carbon” emissions from conversion and degradation of vegetated coastal  
629 ecosystems. *PloS one*, 7(9), e43542.

630 Pethick, J. S. (1981). Long-term accretion rates on tidal salt marshes. *Journal of Sedimentary Research*, 51(2),  
631 571-577.

632 Polidoro BA, Carpenter KE, Collins L, Duke NC, Ellison AM, et al. (2010) The Loss of Species: Mangrove  
633 Extinction Risk and Geographic Areas of Global Concern. *PLoS ONE* 5(4): e10095. doi:10.1371/jour-  
634 nal.pone.0010095

635 R Core Team (2017). A language and environment for statistical computing. R Foundation for Statistical  
636 Computing, Vienna, Austria2014. URL:(<https://www.R-project.org>).

637 Ranjan, R. K., Routh, J., Ramanathan, A. L., & Klump, J. V. (2011). Elemental and stable isotope records of  
638 organic matter input and its fate in the Pichavaram mangrove–estuarine sediments (Tamil Nadu, India). *Ma-  
639 rine Chemistry*, 126(1-4), 163-172.

640 Reynaud, J. Y., Witt, C., Pazmiño, A., & Gilces, S. (2018). Tide-dominated deltas in active margin basins:  
641 Insights from the Guayas estuary, Gulf of Guayaquil, Ecuador. *Marine Geology*, 403, 165-178.

642 Saintilan, N., Rogers, K., Mazumder, D., & Woodroffe, C. (2013). Allochthonous and autochthonous contri-  
643 butions to carbon accumulation and carbon store in southeastern Australian coastal wetlands. *Estuarine,  
644 Coastal and Shelf Science*, 128, 84-92.

645 Schile, L. M., Kauffman, J. B., Crooks, S., Fourqurean, J. W., Glavan, J., & Megonigal, J. P. (2017). Limits  
646 on carbon sequestration in arid blue carbon ecosystems. *Ecological Applications*, 27(3), 859-874.

647 Siikamäki, J., Sanchirico, J. N., & Jardine, S. L. (2012). Global economic potential for reducing carbon di-  
648 oxide emissions from mangrove loss. *Proceedings of the National Academy of Sciences*, 109(36), 14369-  
649 14374.

650 Sturm, K., Werner, U., Grinham, A., & Yuan, Z. (2017). Tidal variability in methane and nitrous oxide emis-  
651 sions along a subtropical estuarine gradient. *Estuarine, Coastal and Shelf Science*, 192, 159-169.

652 Taillardat, P., Friess, D. A., & Lupascu, M. (2018). Mangrove blue carbon strategies for climate change  
653 mitigation are most effective at the national scale. *Biology Letters*, 14(10), 20180251.

654 Temmerman, S., Govers, G., Meire, P., & Wartel, S. (2003). Modelling long-term tidal marsh growth under  
655 changing tidal conditions and suspended sediment concentrations, Scheldt estuary, Belgium. *Marine Geol-*  
656 *ogy*, 193(1-2), 151-169.

657 Temmerman, S., Govers, G., Wartel, S., [and](#) [Meire, P.](#) (2004). Modelling estuarine variations in tidal marsh  
658 sedimentation: response to changing sea level and suspended sediment concentrations: *Marine Geology*, v.  
659 212, p. 1-19.

660 Tue, N.T., Quy, T.D., Hamaoka, H., Nhuan, M.T., [and](#) [Omori, K.](#) (2012) Sources and Exchange of Partic-  
661 ulate Organic Matter in an Estuarine Mangrove Ecosystem of Xuan Thuy National. 1060–1068.

662 Tue, N. T., Dung, L. V., Nhuan, M. T., & Omori, K. (2014). Carbon storage of a tropical mangrove forest in  
663 Mui Ca Mau National Park, Vietnam. *Catena*, 121, 119-126.

664 [Twilley, R. R., Chen, R. H., & Hargis, T. \(1992\). Carbon sinks in mangroves and their implications to carbon  
665 budget of tropical coastal ecosystems. \*Water, Air, and Soil Pollution\*, 64\(1-2\), 265-288.](#)

666 Twilley, R. R., Gottfried, R. R., Rivera-Monroy, V. H., Zhang, W., Armijos, M. M., & Boderó, A. (1998).  
667 An approach and preliminary model of integrating ecological and economic constraints of environmental  
668 quality in the Guayas River estuary, Ecuador. *Environmental Science & Policy*, 1(4), 271-288.

669 Twilley, R. R., Cárdenas, W., Rivera-Monroy, V. H., Espinoza, J., Suescum, R., Armijos, M. M., & Solór-  
670 zano, L. (2001). The Gulf of Guayaquil and the Guayas river estuary, Ecuador. In *Coastal marine ecosystems*  
671 *of Latin America* (pp. 245-263). Springer, Berlin, Heidelberg.

672 Van de Broek, M., Temmerman, S., Merckx, R., & Govers, G. (2016). Controls on soil organic carbon stocks  
673 in tidal marshes along an estuarine salinity gradient. *Biogeosciences*, 13(24), 6611-6624.

674 Van de Broek, M., Vandendriessche, C., Poppelmonde, D., Merckx, R., Temmerman, S., [and](#) [Govers, G.](#)  
675 (2018). Long-term organic carbon sequestration in tidal marsh sediments is dominated by old-aged alloch-  
676 thonous inputs in a macrotidal estuary: *Global Change Biology*, v. 24, no. 6, p. 2498-2512.

677 Weiss, C., Weiss, J., Boy, J., Iskandar, I., Mikutta, R., & Guggenberger, G. (2016). Soil organic carbon stocks  
678 in estuarine and marine mangrove ecosystems are driven by nutrient colimitation of P and N. *Ecology and*  
679 *evolution*, 6(14), 5043-5056.

680 Więski, K., Guo, H., Craft, C. B., & Pennings, S. C. (2010). Ecosystem functions of tidal fresh, brackish, and  
681 salt marshes on the Georgia coast. *Estuaries and Coasts*, 33(1), 161-169.

682 Yee, S. (2010). REDD and BLUE carbon: carbon payments for mangrove conservation.

683

684

685

686

687

688

689

690

691

692

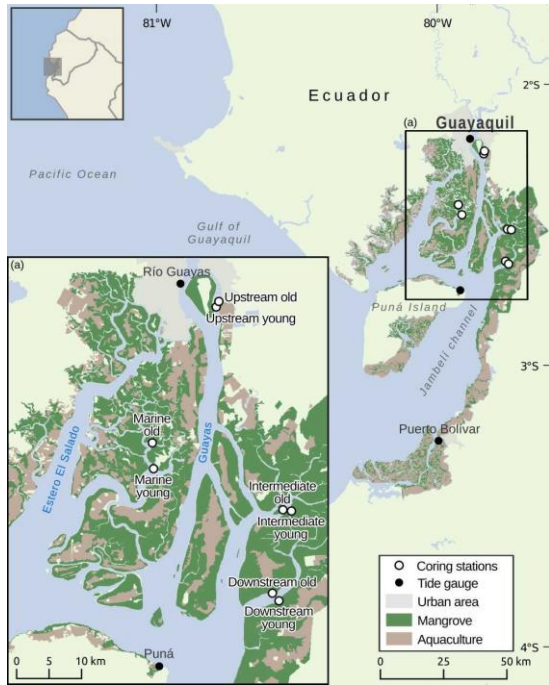
693

694

695

696

697



698

699 **Figure 1** Map of the Guayas Delta showing the locations of the sampled young and old mangrove systems along  
700 an estuarine land-to-sea gradient.

701

702

703

704

705

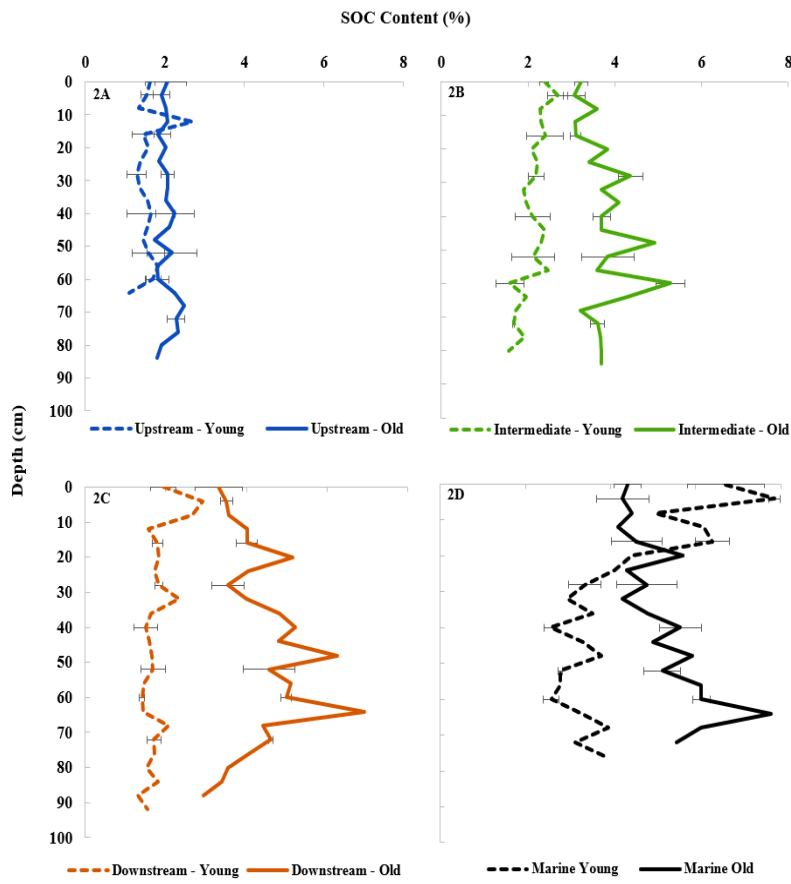
706

707

708

709

710



711

712 **Figure 2** Depth profiles of SOC content (%) for all sites. Fig.2A: Upstream Zone; Fig.2B: Intermediate  
713 Zone; Fig.2C: Downstream Zone; Fig.2D: Marine Zone. Data points show the average OC% of sediment  
714 samples from three replicate cores per site and error bars for specific points represent the standard deviation.

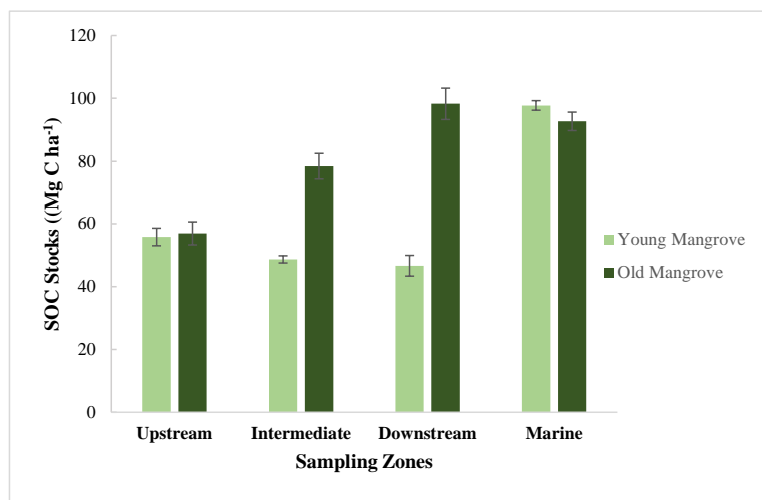
715

716

717

718

719



728

729 **Figure 3** Total sediment organic carbon (SOC) stocks (Mg C ha<sup>-1</sup>) for the upper 0.64 m of the vertical  
730 sampling profiles. Standard deviation was calculated based on the SOC stocks of three replicate cores per  
731 site.

732

733

734

735

736

737

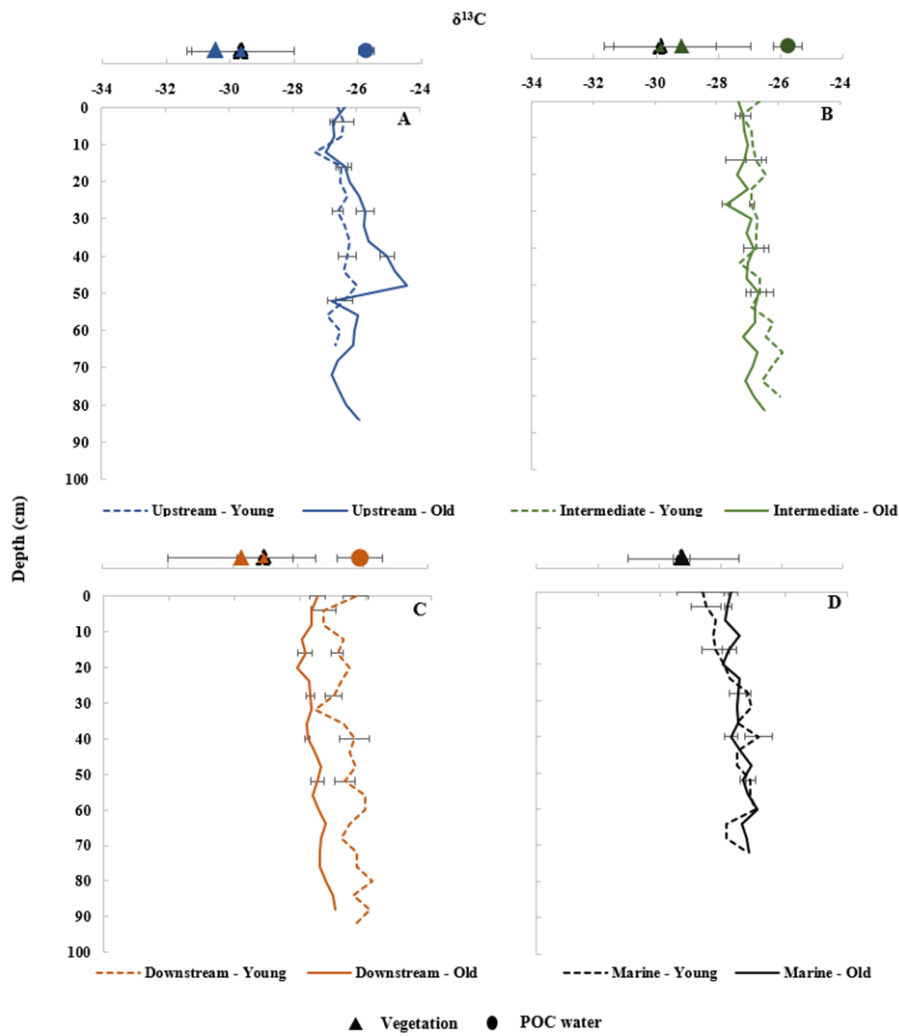
738

739

740

741

742



743

744 **Figure 4** Depth profiles of  $\delta^{13}\text{C}$  of sediment cores and  $\delta^{13}\text{C}$  of autochthonous above and belowground veg-  
745 etation (triangles) and allochthonous POC (circles) of adjacent water bodies for the sites (values are provided  
746 in Table S2, S4 and S5). Fig.4A: Upstream Zone; Fig.4B: Intermediate Zone; Fig.4C: Downstream Zone;  
747 Fig.4D: Marine Zone. Average POC data in dry and wet seasons (both high and low tides) were used. POC

748 data are considered representative for the water flooding both the adjacent young and old sites in each zone.  
749 Vegetation data represent average values for roots, sun-shaded and sun-exposed green leaves, senescent  
750 leaves, leaf litter, live twigs, and branches, per young and old site in each zone. No data on POC and vegeta-  
751 tion were obtained for the Marine site. Error bars represent the standard deviation of sediment subsamples  
752 taken at 0.04m depth increment for the three replicate cores and 8 types of vegetation samples (see Section  
753 2.2.) taken per site and 8 POC samples taken per sampling zone.

754

755

756

757

758

759

760

761

762

763

764

765

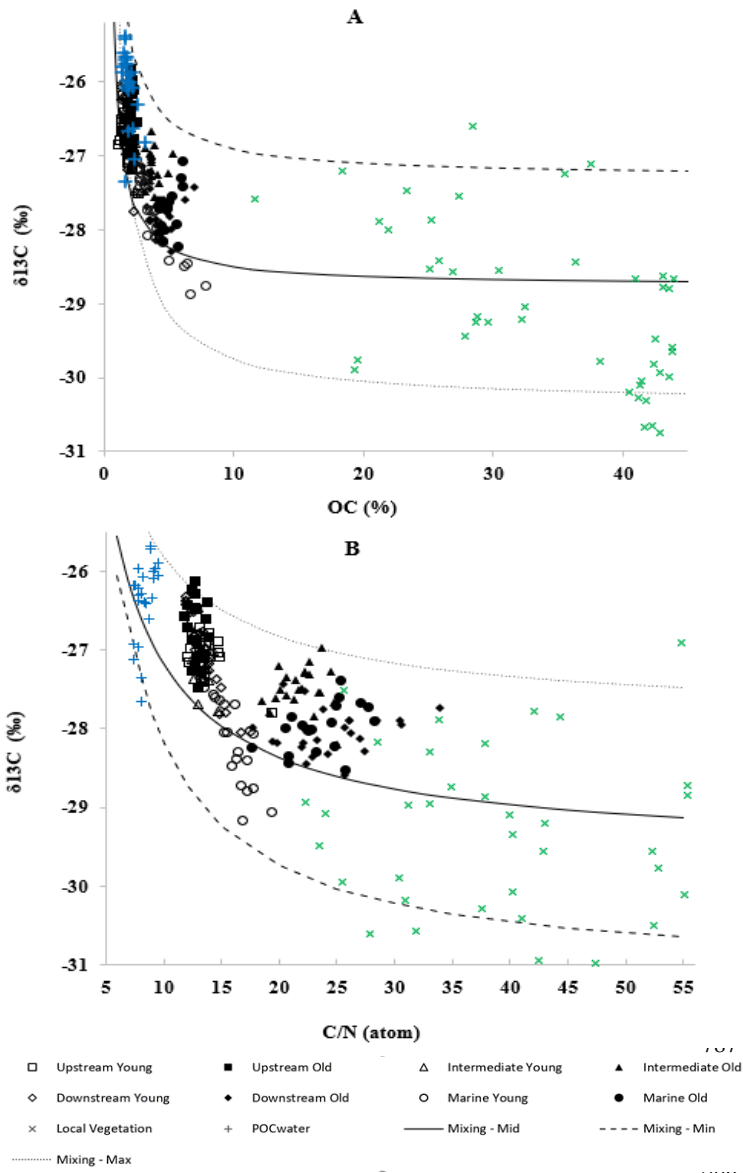
766

767

768

769

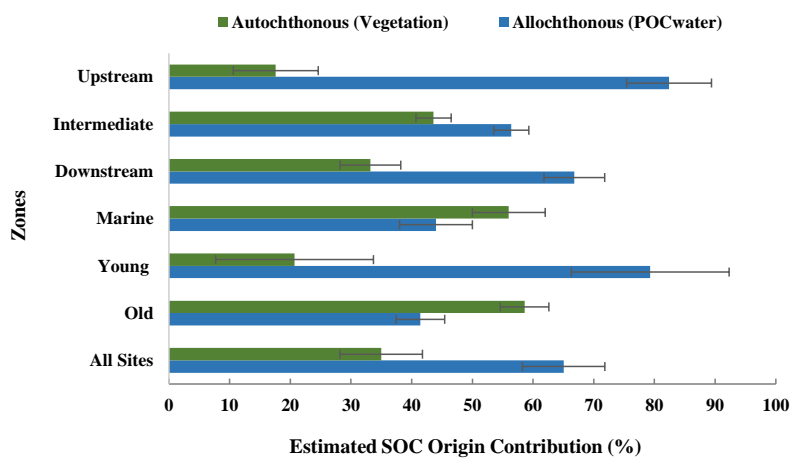
770



789

791 **Figure 5 (A)** Stable carbon isotope ratios  $\delta^{13}\text{C}$  (‰) versus SOC content (%) and **(B)**  $\delta^{13}\text{C}$  (‰) values versus  
792 C/N (atom) ratios of all sampled sites. Different curves correspond to different end-member values for the  
793 sources (see text for details).

794  
795  
796  
797



808  
809 **Figure 6** Estimated contribution (%) of allochthonous and autochthonous origins to the SOC of the study  
810 sites. Averages and standard deviations were calculated from three replicate cores per site.  
811